Nucleation of $YBa_2Cu_3O_7$ From Precursor Films Using the Barium Fluoride Process

Vyacheslav F. Solovyov, Harold J. Wiesmann, and Masaki Suenaga

***Abstract*—Coated-conductor applications of YBCO require YBCO layers with high J_c and a thickness of several micrometers. The barium fluoride process offers a convenient way of depositing crack-free fluorinated precursor layers up to 5 microns thick. However, converting thick precursor layers into c-axis-oriented YBCO films is challenging due to extensive nucleation of random grains. In this paper we address this problem with both a theoretical and experimental analysis of YBCO nucleation. We utilized optical polarization contrast to observe YBCO nuclei imbedded in the precursor matrix. We observed that the nuclei density strongly depends on processing parameters, with the oxygen partial pressure being one of the strongest factors. During ex-situ processing the nuclei merge and form grains and the nuclei density is, therefore, directly related to the grain size of YBCO film. It is desirable to have a small grain structure, since large grains do not connect well and the J_c of such a film is low. However, attempts to increase the nuclei density also generates more randomly oriented grains. Therefore the optimization of ex-situ processing is essentially finding a balance between c-axis grain density and random grain content.**

***Index Terms*—Barium fluoride process, coated conductors, YBCO.**

I. Introduction

DEVELOPMENT of coated $YBa_2Cu_3O_7$ (YBCO) conductors for magnetic field and electrical utility applications requires a robust technology for growing high quality YBCO epitaxial layers. Ex-situ processing is being considered as a component of such a technology, primarily due to the possibility of parallel processing of large quantities of coated tape [1]. Ex-situ processing is essentially the conversion of a fluorinated precursor into epitaxial YBCO with the release of HF and absorption of water vapor. It is generally now accepted that the growth rate of YBCO is limited by removal of the reaction product, HF, via gaseous diffusion and/or convection [2]. The partial pressure of HF, $P_e(\mathrm{HF})$, at the growth front can be related to the partial pressure of water vapor, $P(\mathrm{H_2O})$, in the processing atmosphere through the equilibrium condition, $P_e(\mathrm{HF}) = K_e P(\mathrm{H_2O})$, where K_e is the equilibrium constant of the precursor $\rightarrow$ YBCO conversion reaction.

The YBCO growth rate, r, is proportional to the HF gas flux:

$$r \propto \frac{P(H_2O)^{1/2} D_g}{W} \tag{1}$$

A very important and still unexplored subject is the nucleation of YBCO in the ex-situ process. Attempts to study the nucleation by means of transmission electron microscopy (TEM) has provided only fragmented information [3], mainly because TEM samples offer a limited field of view and are difficult to prepare. It is essential to know details of the nucleation process, since the YBCO layer inherits the microstructure of the nuclei. In this paper we will briefly outline our latest understanding of the YBCO nucleation mechanism in the ex-situ process and will primarily concentrate on practical aspects of optimization of thick film YBCO performance.

II. Experiment

The precursor films were deposited by high-rate co-evaporation of Y, BaF_2 and Cu in a vacuum chamber at an overall pressure $\sim 10^{-6}$ Torr, described in more detail in [2]. The substrates were buffered Ni-W RABITS tapes provided by AmSC. Finally, the films were processed in a standard atmospheric quartz reactor. The processing atmosphere consisted of oxygen, water vapor and balance nitrogen. We utilized optical polarization contrast to detect YBCO nuclei, which had grown up to the film surface. Careful adjustment of the polarization angle allowed a good contrast to be achieved between the YBCO grains and unreacted precursor. A similar technique was used to bring out the outlines of YBCO grains after the film was completely processed.

Optical images were used to determine average grains size and inter-nuclei spacing. Critical current density was determined from transport I-V curves using a 1 $\mu\mathrm{V/cm}$ field criterion. The transport measurements were performed in liquid nitrogen. The structural characterization comprised standard 2-theta diffraction and texture analysis using 4-circle goniometry.

III. Results

Fig. 1(a) shows the polarization contrast of the surface of a 0.2 μm thick YBCO film deposited on buffered RABITS tape and processed for 10 min under the following conditions: $P(\mathrm{O_2}) = 100$ milliTorr, $P(\mathrm{H_2O}) = 50$ Torr, $T = 735^{\circ}\mathrm{C}$, atmospheric pressure. Dark circles are YBCO nuclei and the rest of the area is unprocessed fluorinated precursor. We have traced the grain boundaries of the Ni-W tape with solid white lines for clarity. This figure illustrates the complexity of the microstructure of ex-situ processed films. The network of YBCO grains is superimposed over the much larger grains of the textured metal base.

Manuscript received October 3, 2004. This work was supported by the U.S. Department of Energy under contract no. DE-AC02-98CH10886.

The authors are with Brookhaven National Laboratory, Upton, NY 11973 USA (e-mail: www.bnl.gov/msd/).

Digital Object Identifier 10.1109/TASC.2005.847762

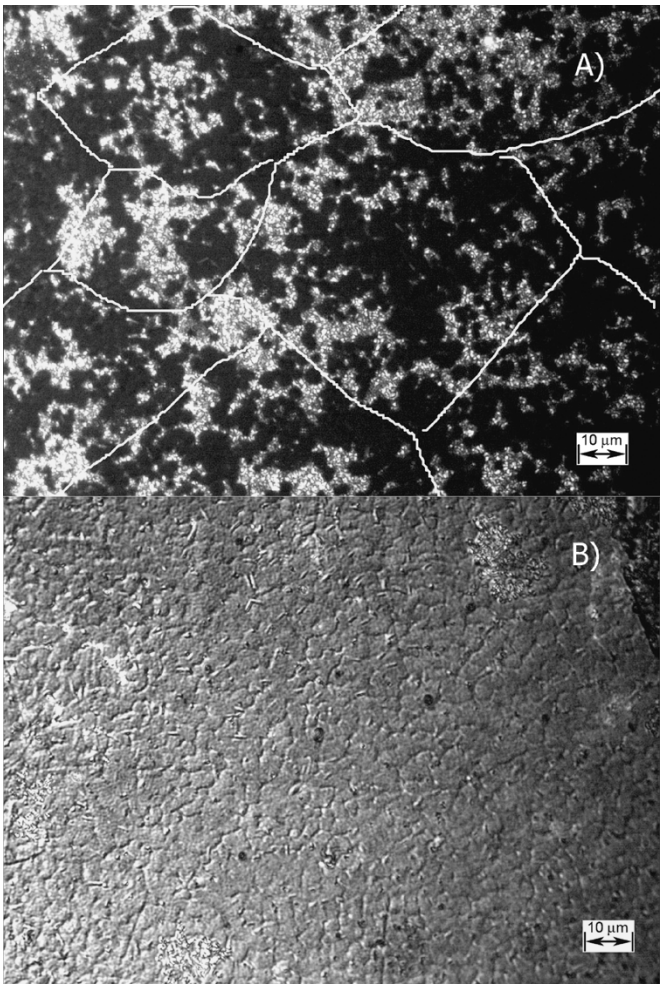

Fig. 1. Optical polarization contrast of surface of 0.2 μm thick film. Panel A, the film was quenched after 10 min of processing. YBCO nuclei can be clearly seen as dark circles. Grain boundaries of underlying Ni-W tape are traced with white lines for clarity. Panel B, the same film completely processed. Note granular surface morphology.

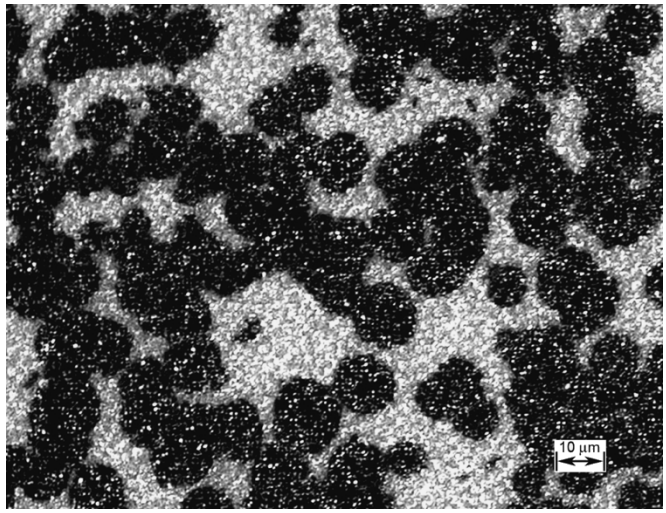

Fig. 2. Optical polarization contrast of surface 2 μm precursor film showing YBCO nuclei (dark discs). The film was processed under conditions identical to one shown in Fig. 1 for 0.5 hr. Note substantial reduction of the nuclei density as compared with Fig. 1.

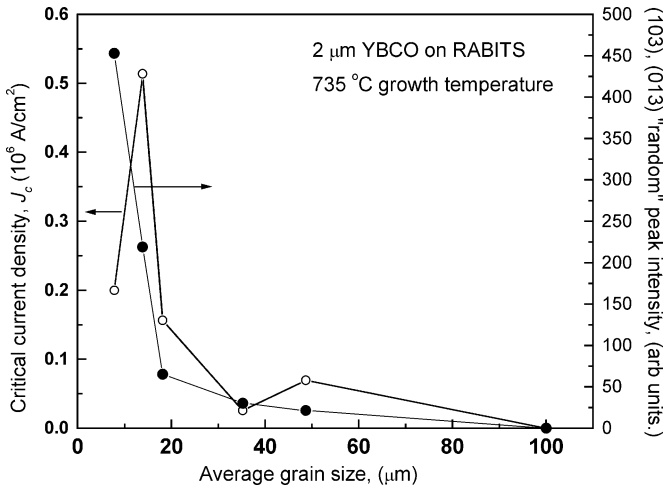

Fig. 3. Critical currents and intensity "random" peak of 2 μm thick YBCO films on RABITS buffered tape vs. the grain size.

Fig. 1(b) shows the surface of the same film after processing was completed and the nuclei merged forming a coarse grained film. This kind of granularity seems to be a typical feature of ex-situ grown films. The film shown in Fig. 1(b) had a negligible J_c. Using magneto-optic imaging we established that the large grains were not well coupled even though the in-plane and out-of-plane grain alignment was good. While the cause of this effect is under investigation, the most likely explanation is that secondary phases get trapped between merging growth fronts. Since the amount of secondary phases accumulated by the growth front is proportional to the growth front travel distance, the de-coupling is more pronounced when the average grain size is large. Taking into account very the short coherence length of YBCO, it is not surprising that even thin nonsuperconducting layers can effectively de-couple even though the YBCO grains are almost perfectly aligned.

Films at 2 microns thick processed under the same conditions tended to have much larger c-axis oriented grains. An example of this effect shown in Fig. 2, which shows the surface of 2 μm thick film processed under conditions identical to those of the 0.2 μm sample shown in Fig. 1. Comparing of Figs. (1a) and 2 one notes the remarkable reduction of the c-axis oriented nuclei density in the thicker film.

It is possible to control the nuclei density and resulting grain size. In a forthcoming publication [4] we analyze factors that influence the nuclei density and, consequently, the grain size. Briefly, the strongest factors are the growth rate and oxygen partial pressure. For example, we processed a 0.2 μm thick film under conditions identical to the sample shown in Fig. 1 except that the oxygen partial pressure was increased to 300 milliTorr. This caused the gain size to decrease below the optical resolution of our microscope and the grain network shown in Fig. 1(b) disappeared. However, J_c increased to 1.2 $\mathrm{MA/cm^2}$.

Fig. 3 illustrates the results of our optimization effort for a set of 2 μm thick precursor films on buffered RABITS Ni-W tapes. These films were processed at atmospheric pressure, 735°C, $P(\mathrm{H_2O}) = 70$ Torr, the oxygen partial pressure was varied from 100 to 300 milliTorr with the growth rate ranging from 0.04 to 0.14 nm/s. The plot shows critical current density and the intensity of "random" peaks as a function of grain size, which

for each sample was determined from optical images similar to the one shown in Fig. 1(b). We started the optimization with a very large-grained film, gain size $\sim$ 100 μm, processed at $P(O2) = 100$ milliTorr and a growth rate of 0.04 nm/s. As we decreased the grain size by raising $P(O_2)$ J_c gradually increased due to the improved coupling of the smaller grains. When the grain size approached 10 microns we observed extensive nucleation of random grains, evidenced by the rise of the intensity of (103)-(013) reflections. Beyond this point the critical current plummeted, because random grains negated all of the gain in J_c from the improved coupling of the c-axis oriented grains. For this specific precursor-substrate combination the maximum J_c that we could achieve was 0.6 MA/cm^2. However, using a different substrate we could make the grain size as small as 5 μm with $J_c = 1.1$ MA/cm^2 for a 2 μm thick film. One can summarize our experience with the ex-situ processing of thick BaF_2-based precursor films by saying that optimization means maximizing the density of c-axis oriented grains while keeping the density of random grains to a minimum.

Fortunately the inter-grain coupling is more tolerant to the grain size in thicker films. As we mentioned before the 0.2 μm thick film shown in Fig. 1 had a grain size 5 μm and was completely uncoupled, while according to Fig. 3, a 2 μm thick film with 10 μm grains had a reasonably high J_c. We have no understanding at this point why the inter-grain coupling is thickness dependent.

IV. Discussion

Ex-situ processing comprises two distinct thermodynamic events: nucleation and growth. During the nucleation stage YBCO nuclei appear on the precursor-substrate interface. The nuclei start to grow and eventually coalesce into a more or less uniform YBCO layer. To be stable the nuclei have to overcome an energy barrier. The height of the barrier is the sum of the positive surface energy and negative volume energy of the nucleus. The substrate provides areas with lower surface energy thus facilitating nucleation. The volume contribution is described by the supersaturation (or driving force), $s = \delta\mu/kT$, which is a measure of the deviation of the thermodynamic potential of a reaction, $\delta\mu$, from equilibrium. When $\delta\mu = 0$ then $s = 0$. In our case the deviation from equilibrium is measured by the difference of the HF partial pressure at any point on the precursor-substrate interface from the equilibrium HF pressure, $P_e(HF)$.

The surface energy depends on the nucleus orientation with respect to the substrate. Randomly oriented nuclei have a surface energy higher than c-axis oriented nuclei. Therefore the initiation of random nucleation requires levels of supersaturation higher than that required for c-axis nucleation. Without modifying the substrate, adjusting the level of supersaturation is the only way to selectively nucleate the c-axis oriented grains.

To estimate the supersaturation, consider the geometry shown in Fig. 4. Here we have a precursor of thickness d, with existing nuclei at the positions labeled A and a potential nucleation site at position B. Positions A represent nucleation sites with a reduced surface energy. C-axis oriented nuclei occupy these sites first. Position B represents a site with higher surface energy, which, depending on the level of supersaturation, can be occupied by either a random or c-axis oriented nucleus. As the existing nuclei at positions A grow they release HF. The HF diffuses through the precursor thickness, d, (with a permeability D_s) and then through the gaseous atmosphere (with permeability D_g) over the length W. The partial pressure of HF at the surface of the nuclei is equal to the equilibrium value $P_e(HF)$ and is assumed to drop to zero at a distance W from the film surface. Since $D_s \ll D_g$ we can neglect $P(HF)$ gradients at the film surface. If so, $P_B(HF)$, which is the partial pressure of HF at position B in Fig. 4, would be equal to $P_e(HF) - \delta P(HF)$, where $\delta P(HF)$ is the pressure drop of HF across the precursor solid. We can estimate $\delta P(HF)$ from the argument that the HF flux is the same in the gas and the solid and that $\delta P(HF) \ll P_e(HF)$, so $\delta P(HF) D_s/d = P_e(HF) D_g/W$. Using (1) we find the supersaturation at position B:

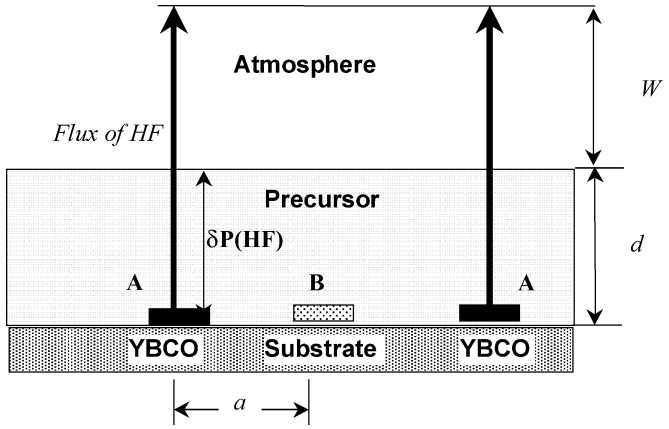

Fig. 4. Geometry used in calculation of supersaturation for a precursor film of thickness d. Existing YBCO nuclei are labeled A and potential nucleation site is labeled B.

$$s = -\ln\left(\frac{P_B(HF)}{P_e(HF)}\right) \approx -\frac{dD_g}{WD_s} \propto \frac{dr}{P(H_2O)^{1/2}D_s} \qquad (2)$$

Examining (2) we see that increasing the thickness of the precursor elavates the supersaturation making thicker films more prone to random nucleation. To decrease the supersaturation we need to compensate for the increased thickness. The equation suggests several ways to counter-balance the "thickness" term, d, such as slowing down the growth rate, r, or increasing $P(H_2O)$ and/or the film permeability, D_s.

Estimation of the surface energy of the nuclei is more difficult, since many essential parameters are unknown. The substrate morphology reflects the catalyzing potency of the substrate, for instance the $SrTiO_3$ (100) crystal face is capable of providing far more nucleation sites than a technical oxide buffer.

As previously discussed oxygen partial pressure has a remarkably strong effect on nucleation [4]. This is surprising taking into account that the growth rate itself is practically independent on $P(O_2)$ [2]. We speculate that the nuclei have an oxygen stoichiometry somewhat different from that of bulk YBCO, making the nuclei surface energy sensitive to $P(O_2)$.

Overall the nucleation energy would include the volume term, (2), and the surface energy term which would strongly depend on $P(O_2)$ and the substrate type.

Reduced $P(O_2)$ was successfully used for processing of c-axis oriented 0.4 μm thick films as early as 1991 [5]. However for processing of 5 μm thick films we had to use a very high $P(H_2O)$ in addition to a low $P(O_2)$ [6]. However, $P(O_2)$ cannot be made too low without inducing excessive cation disorder in the YBCO structure. This puts an emphasis upon increasing D_s, i.e. making the precursor more permeable for HF, as an effective way to compensate for the d term in (2).

We can now come up with a simple interpretation for our results shown in Fig. 3. By increasing $P(O_2)$ we reduced the barrier for nucleation, nucleating more c-axis oriented nuclei, with an increasing grain density and higher J_c as the result. At some point increasing the $P(O_2)$ level causes the barrier for nucleation to be decreased to such a degree that the c-axis versus random grain selectivity is lost. Even though the grain size is still decreasing the fraction of randomly oriented grains increases causing J_c to decrease as shown in Fig. 3.

Equation (2) predicts that thicker films will have increased supersaturation and should have smaller grains. However, as illustrated by Figs. 1 and 2 grains in a thicker film are larger. We believe that to understand this effect we should consider the dynamics of nuclei ripening. We use Fig. 4 to illustrate one possible scenario. When nuclei first form at low-energy positions, A, they experience fast growth, since the area of the growth front associated with them is small. Therefore, these nuclei have a chance to grow to the surface before other higher-energy locations, like the one labeled B, become occupied by YBCO. Once the growth front of a nuclei reaches the surface at position A, the $P(HF)$ at the film surface would be very close to $P_e(HF)$ and the pressure drop, $\delta P(HF)$, across the film thickness will vanish. This will cause the supersaturation at position B to drop substantially and the growth rate of nuclei at position B would be reduced by a factor $\propto aD_s/dD_g$. The consequence of this nucleation-ripening scenario is that B nuclei will never reach the surface and will be overgrown by A nuclei. This also may be an explanation for several TEM sightings of unprocessed precursor which appears to be trapped between YBCO layers [3]. As we can see the film thickness and the precursor permeability are the negative factors which equally contribute to undesirable grain coarsening.

V. Conclusion

Supersaturation can be used as a single optimization parameter in the YBCO ex-situ process. Optimizing the value of the supersaturation allows one to maximize the density of c-axis oriented nuclei while keeping number of randomly oriented grains to a minimum.

Acknowledgment

The authors greatly appreciate the American Superconductor Corp. for providing RABITS substrates for this study.

References

[1] D. T. Verebelyi *et al.*, "Uniform performance of continuously processed MOD-YBCO-coated conductors using a textured Ni-W substrate," *Supercond. Sci. Technol.*, vol. 16, pp. L19–L22, Mar. 2003.

[2] V. F. Solovyov, H. J. Wiesmann, and M. Suenaga, "Growth rate limiting mechanisms of $YBa_2Cu_3O_7$ films manufactured by ex-situ processing," *Physica C*, vol. 353, pp. 269–274, May 2001.

[3] P. C. McIntyre, M. J. Cima, and A. Roshko, "Epitaxial nucleation and growth of chemically derived $Ba_2YCu_3O_{7-x}$ thin films on (001) $SrTiO_3$," *J. Appl. Phys.*, vol. 77, pp. 5263–5272, May 1995.

[4] V. F. Solovyov, H. J. Wiesmann, and M. Suenaga, "Nucleation of $YBa_2Cu_3O_{7-x}$ on buffered metallic substrates in thick precursor films made by the BaF_2 process," *Supercond. Sci. Technol.*, submitted for publication.

[5] R. Feenstra, T. B. Lindemer, J. D. Budai, and M. D. Galloway, "Effect of oxygen pressure on the synthesis of $YBa_2Cu_3O_{7-x}$ thin films by post-deposition annealing," *J. Appl. Phys.*, vol. 69, pp. 6569–6585, May 1991.

[6] V. F. Solovyov *et al.*, "High rate deposition of 5 μm thick $YBa_2Cu_3O_7$ films using the BaF_2 ex-situ post annealing process," *IEEE Trans. Appl. Supercond.*, vol. 9, pp. 1467–1470, Jun. 1999.